PROCEEDINGS OF SCIENCE

Optical Properties of the Fluorescence Detector in the Telescope Array Experiment Using the Opt-copter

PoS(ICRC2025)330

Aoi Matsuzawa,[a,*] **Takayuki Tomida,**[a] **Daiki Sato,**[a] **Yuichiro Tameda,**[b] **Daisuke Ikeda,**[c] **John Matthews**[d] **and Telescope Array Collaboration**

[a] *Academic Assembly School of Science and Technology Institute of Engineering, Shinshu University, Nagano, Nagano, Japan*

[b] *Department of Engineering Science, Faculty of Engineering, Osaka Electro-Communication University, Neyagawa, Osaka, Japan*

[c] *Faculty of Engineering, Kanagawa University, Yokohama, Kanagawa, Japan*

[d] *High Energy Astrophysics Institute and Department of Physics and Astronomy, University of Utah, Salt Lake City, UT, USA*

E-mail: 24w6070e@shinshu-u.ac.jp

The Opt-copter was developed as a calibration device for the FDs. The Opt-copter is equipped with a UV LED light source and a Real-Time Kinematic GPS (RTK-GPS) module for precise positioning. Using the Opt-copter, the pointing direction analysis of all 38 TA-FDs at the three stations has been completed using the Opt-copter. As a result, the elevation shifts showed different tendencies at each station. Similar shifts were observed among FDs pointing in similar directions, even if located at different stations about 35 km apart. This suggests that systematic effects may have been introduced by the types and motions of stars observed by FDs. The overall uncertainty of this analysis was estimated to be 0.03°.

39th International Cosmic Ray Conference (ICRC2025)
15–24 July 2025
Geneva, Switzerland

ICRC 2025
The Astroparticle Physics Conference
Geneva July 15-24, 2025

[*] Speaker

1. Introduction

The Telescope Array (TA) experiment, located in Utah, USA, aims to observe ultra-high-energy cosmic rays (UHECRs) with energies exceeding 10^{18} eV. Three fluorescence detector (FD) stations capture ultraviolet fluorescence light emitted by nitrogen molecules in the atmosphere when air showers develop. Figure 1a shows the site map of the TA experiment and the locations of the FD stations. Figure 1b shows the conceptual diagram of a TA FD unit.

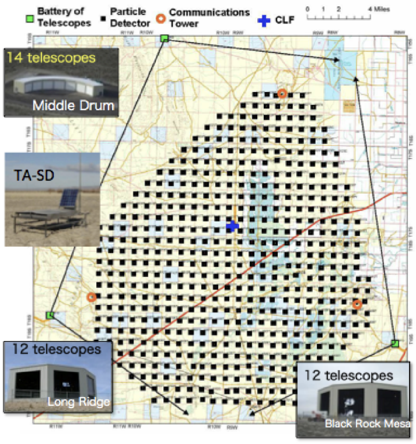

(a) Site map of the TA, showing the appearance of each FD station. Black squares represent surface detectors, green squares indicate FDs, and a blue cross denotes the CLF.

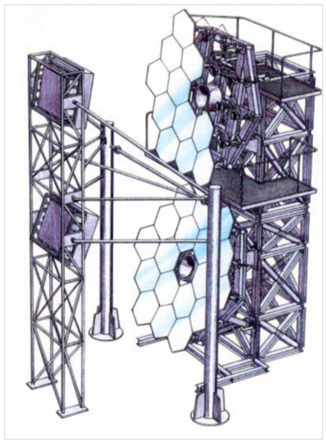

(b) Conceptual diagram of the TA FD.

Figure 1: Overview of the TA experiment and the TA FD.

The TA detectors have been operating for over 20 years, and improved precision is increasingly required. In conventional FD's pointing direction analysis, the pointing direction is determined by comparing the positions of stars observed by the FD with those listed in star catalogs [1]. Accurate calibration of the optical properties of the FDs is essential for estimating the energy and composition of primary cosmic rays using FD data. The "Opt-copter" was developed as an unmanned aerial vehicle (UAV) equipped with a UV LED light source and a Real-Time Kinematic GPS (RTK-GPS) for precise positioning [2]. Using this system, we can obtain detailed information about the optical properties of all FD stations, which are located at three sites, each approximately 35 km apart. The pointing directions of the 12 FDs at the BRM station have already been analyzed [3]. In this paper, we present the results of the pointing direction analysis and its accuracy for 26 TA-FDs.

2. The Opt-copter

The purpose of the Opt-copter is to analyze the optical properties of the FD. The copter is equipped with a Real-Time Kinematic GPS (RTK-GPS) module for precise positioning and a UV light source. The timing of both the positioning and light emission is synchronized using the one-pulse-per-second (PPS) signal from the GPS. This system serves as a light source with a known position and can fly within the field of view (FoV) of the FD. This system allows us to analyze the FD's pointing direction and image size by comparing the position of the light source measured by RTK-GPS with the position of the light source observed by the FD. Figure 2a shows the appearance of the Opt-copter. Figure 2b shows a schematic view of the Opt-copter operation.

(a) Appearance of the Opt-copter. (b) Schematic view of the Opt-copter operation.

Figure 2: Overview of the Opt-copter.

2.1 Real-Time Kinematic GPS (RTK-GPS)

Since the calibration accuracy strongly depends on how precisely the light source position is measured, the Opt-copter is equipped with an RTK-GPS module for high-precision positioning. To achieve a pointing calibration of the photomultiplier tubes (PMTs) with an accuracy of 0.1°, a positioning accuracy of 0.5 m is required. This level of precision is made possible by employing an RTK-GPS system (Piksi, Swift Navigation, Fig. 3). The RTK-GPS system uses two GPS modules and determines their relative position based on the phase difference of signals transmitted from GPS satellites. The typical positioning accuracy of RTK-GPS is better than 10 cm, which corresponds to an angular accuracy of 0.02° in the FD's pointing direction.

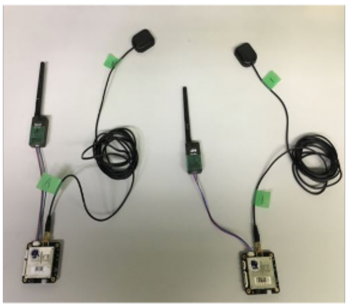

Figure 3: RTK-GPS module.

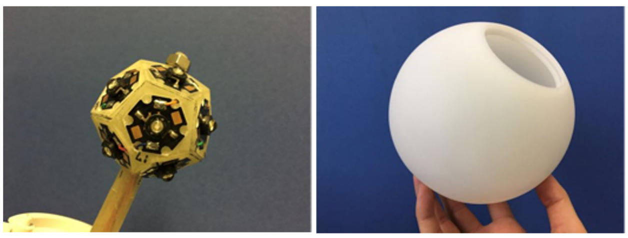

Figure 4: Left: 12 UV-LEDs. Right: spherical diffuser.

2.2 UV-LED light source

The optical system of the FD is optimized for photons in the wavelength range of 300-400 nm, corresponding to the fluorescence light emitted by nitrogen and oxygen molecules. As a light source, we employ twelve UV-LEDs (H2A1-H375-E, Roithner Lasertechnik) with a central wavelength of 375 nm. Since each LED exhibits a highly anisotropic emission pattern, a spherical light diffuser is used to achieve isotropic emission (see Fig. 4). The LEDs are attached to each face of a dodecahedron fabricated using a 3D printer, and the entire assembly is enclosed within a diffuser.

3. Data set and analysis method

$$(\Delta\theta, \Delta\phi) = (\theta_{\mathrm{GPS}}, \phi_{\mathrm{GPS}}) - (\theta_{\mathrm{CoG}}, \phi_{\mathrm{CoG}}) \qquad (1)$$

θ is the azimuth angle in the FD's FoV, and ϕ is the elevation angle in the same coordinate system. The RTK-GPS measures the relative position of the rover with respect to a base station installed on a survey marker. $(\theta_{\mathrm{GPS}}, \phi_{\mathrm{GPS}})$ is the light source position measured by RTK-GPS, converted into the azimuth and elevation angles in the FD's coordinate system. As shown in Fig. 5, each PMT in the FD produces a signal. When light enters the PMT, the output voltage increases. This voltage is then digitized by an Analog-to-Digital Converter (ADC) and recorded as ADC values. Fig. 6 shows the assumed pointing directions of all PMTs in a single FD unit.

$$(\theta_{\mathrm{CoG}}, \phi_{\mathrm{CoG}}) = \frac{\sum_{i=0}^{N_{\mathrm{PMT}}} (\theta_{\mathrm{PMT}_i}, \phi_{\mathrm{PMT}_i}) \cdot N_{pe_i}}{\sum_{i=0}^{N_{\mathrm{PMT}}} N_{pe_i}} \qquad (2)$$

N_{PMT} is the PMT ID, $N_{\mathrm{pe},i}$ is the detected light amount (number of photoelectrons) recorded by i-th PMT, and $(\theta_{\mathrm{PMT}_i}, \phi_{\mathrm{PMT}_i})$ is the assumed pointing direction of i-th PMT. The coordinates $(\theta_{\mathrm{CoG}}, \phi_{\mathrm{CoG}})$ is the position of the light source observed by the FD, obtained as the center of gravity (CoG) of these PMT pointing directions, weighted by their detected light amounts.

Fig. 6 shows the event display for a single event. $(\Delta\theta, \Delta\phi)$ is defined as the difference between the light source position measured by the RTK-GPS and that observed by the FD. In the case where the PMT size is negligible compared to the spot size, $(\Delta\theta, \Delta\phi)$ directly corresponds to the shift in the pointing direction.

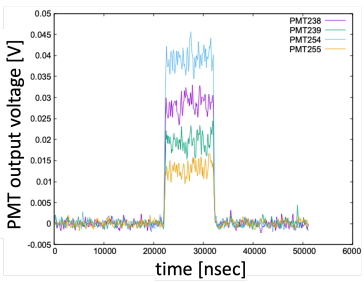

Figure 5: PMT output.

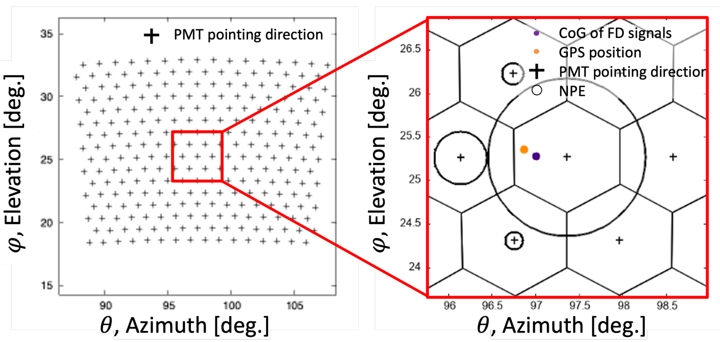

Figure 6: Left: PMT pointing directions. Right: event display.

However, each PMT subtends an angle larger than 1° within the FoV, so the light-source position observed by the FD is biased toward the center of the illuminated PMTs. Fig.7 shows an

FD with a spot size larger than the PMT pitch. In this case, many PMTs are illuminated, and the observed CoG closely follows the position measured by RTK-GPS, resulting in a smooth and nearly linear trajectory in the azimuthal direction. In contrast, Fig.8 shows an FD with a spot size smaller than the PMT pitch. When only one PMT is illuminated, the observed CoG is recorded at the PMT center, resulting in a step-like trajectory in the azimuthal direction. Due to this finite PMT size, the per-event difference between the RTK-GPS and the observed CoG cannot directly determine the true pointing shift. Therefore, the data are statistically processed to minimize the bias toward the PMT centers as much as possible.

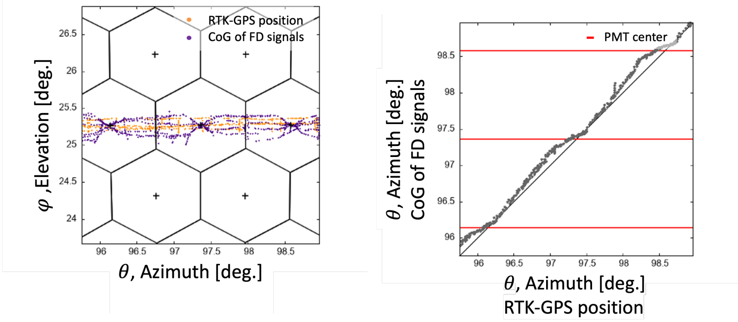

(a) Data extracted from a band centered on the PMT direction (Long Ridge FD 08).

(b) CoG trajectory (Long Ridge FD 08).

Figure 7: Characteristics of the light-source position measured by RTK-GPS and the CoG of the FD signals for a large spot size

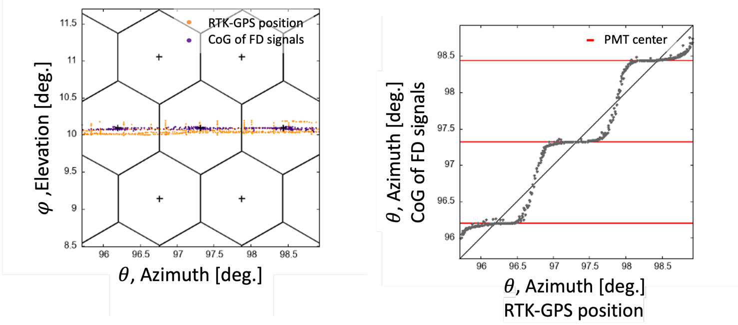

(a) Data extracted from a band centered on the PMT direction (Long Ridge FD 09).

(b) CoG trajectory (Long Ridge FD 09).

Figure 8: Characteristics of the light-source position measured by RTK-GPS and the CoG of the FD signals for a small spot size

$$\overline{(\Delta\theta, \Delta\phi)} = \frac{\sum_{j=1}^{N_{\rm Data}} \left((\theta_{{\rm GPS}_j}, \phi_{{\rm GPS}_j}) - (\theta_{{\rm CoG}_j}, \phi_{{\rm CoG}_j}) \right)}{N_{\rm Data}} \quad (3)$$

Fig. 9 shows the data used for the analysis. To ensure symmetry, data are selected within ±1.5° of the center of the target PMT. Additionally, to reduce the influence of optical aberrations, only data near the center of the FD's FoV are used in the analysis.

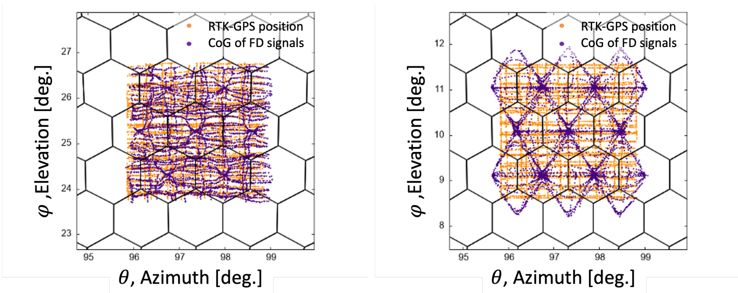

(a) FD with a large spot size (Long Ridge FD 08).

(b) FD with a small spot size (Long Ridge FD 09).

Figure 9: The position of the light source measured by RTK-GPS and the CoG of the FD signals

4. Results

The pointing directions of all 38 FDs at the three stations were analyzed. Fig. 10a shows the differences between the light-source position measured by RTK-GPS and the CoG positions observed by the FD for a case with a large spot size, along with their mean values. Fig. 10b presents the same for a case with a small spot size. When the spot size is smaller, the CoG tends to be more biased toward the center of the PMT, resulting in a larger scatter in the differences. However, even in the case of a large spot size, the standard error of the mean is 0.002°. For Long Ridge FD 08, the actual pointing direction was found to be shifted by -0.09° in azimuth and +0.05° in elevation from the assumed direction, while for Long Ridge FD 09, the shifts were -0.02° in azimuth and +0.02° in elevation.

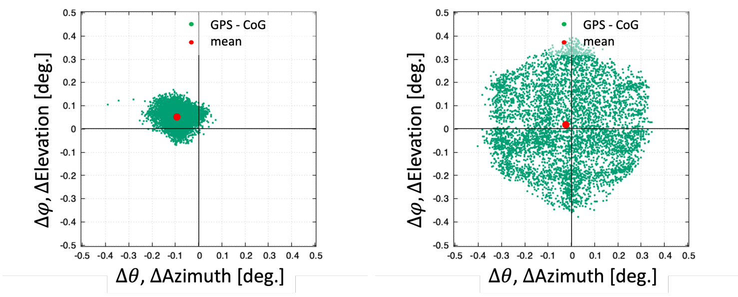

(a) FD with a large spot size (Long Ridge FD 08).

(b) FD with a small spot size (Long Ridge FD 09).

Figure 10: The differences between the RTK-GPS position and the CoG position.

Table 1a is the result for the Long Ridge (LR) station, and Table 1b is that for the Middle Drum (MD) station. The average pointing direction shifts for the LR FDs are -0.03° in azimuth and -0.01° in elevation, while the shifts for the MD FDs are +0.0° in azimuth and +0.20° in elevation. The shifts in azimuth for the two stations are within the analysis accuracy of 0.03°, but the shifts in elevation differ significantly between the two stations.

Fig. 11 shows the FoV of each FD on the x-axis, with 0° corresponding to north, and the shift

Table 1: Pointing direction shift of the FDs analyzed using the Opt-copter.

(a) Long Ridge Station

CAMID	00	01	02	03	04	05	06	07	08	09	10	11
Δ Azimuth [deg.]	-0.02	+0.01	-0.07	+0.01	-0.04	0.00	-0.09	+0.03	-0.09	-0.02	-0.09	-0.03
Δ Elevation [deg.]	-0.12	-0.10	-0.05	-0.10	-0.03	0.00	+0.01	+0.03	+0.05	+0.02	+0.06	+0.13
# of data	5743	7455	2902	3028	2160	3847	4183	4312	5492	5320	3210	5360

(b) Middle Drum Station

CAMID	01	02	03	04	05	06	07	08	09	10	11	12	13	14
Δ Azimuth [deg.]	+0.03	-0.02	+0.10	+0.01	+0.06	+0.01	+0.04	+0.03	+0.07	-0.02	-0.01	0.00	+0.03	-0.10
Δ Elevation [deg.]	+0.14	+0.15	+0.07	+0.17	+0.11	+0.14	+0.19	+0.19	+0.18	+0.20	+0.22	+0.21	+0.23	+0.25
# of data	1434	759	1117	893	1566	898	1297	2881	1181	987	1635	1486	877	1664

in pointing direction on the y-axis. Although each FD station is located more than 35 km apart, the elevation shifts observed in the FDs at the LR and MD stations lie on a continuous trend. This indicates that the pointing direction shifts depend on the direction in which each FD is facing. In other words, this suggests that the types and motions of stars used in conventional star-based pointing calibrations may have introduced systematic effects in the results.

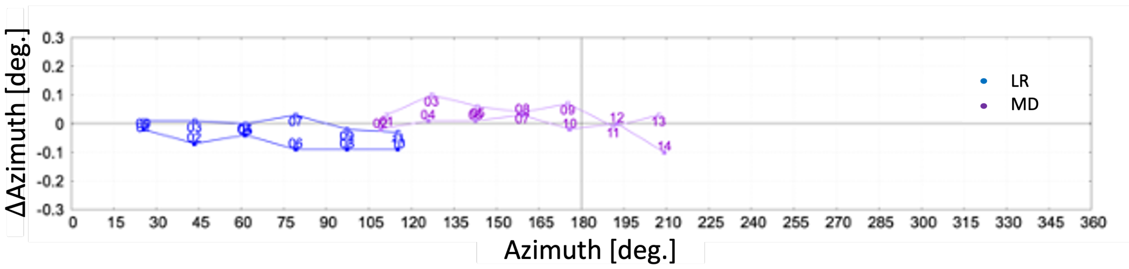

(a) Results of the pointing direction shift in azimuth at LR and MD stations.

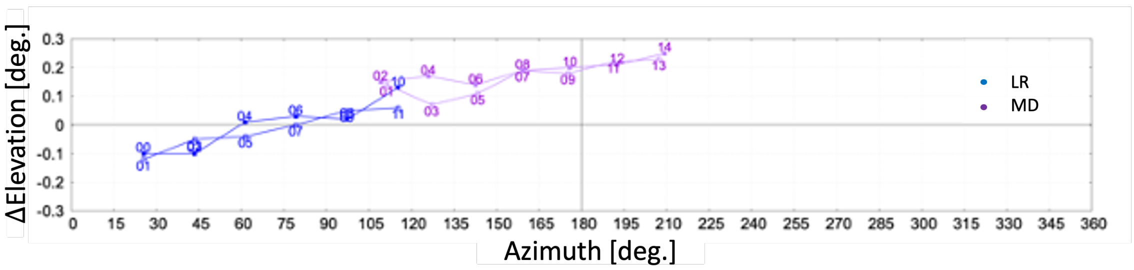

(b) Results of the pointing direction shift in elevation at LR and MD stations.

Figure 11: Results of the shift in the pointing direction of each FD.

The systematic error from the RTK-GPS is estimated to be 0.02°, and the error due to optical aberration is also estimated to be 0.02°. Therefore, the overall accuracy of the analysis results is 0.03°. The difference between the results obtained in 2023 and 2024 falls within 0.03°, indicating no pointing shift due to aging. Furthermore, even when flights were conducted from different survey markers, the difference in analysis results remained within 0.03°, suggesting no misalignment of the survey markers.

5. Conclusion

The pointing direction analysis of all 38 TA-FDs at the three stations has been completed using the Opt-copter. By comparing the light source positions measured by RTK-GPS with the CoG positions observed by FD, the shifts in the FD's pointing directions were evaluated. The results show that the azimuthal shifts are small across all stations, while the elevation shifts vary significantly depending on the FD orientation. Similar elevation shifts were observed among FDs pointing in the same direction, even if located at different stations, indicating a potential systematic effect introduced by the types and motions of stars used in previous calibrations. Conventional calibrations assumed pointing accuracy of $\pm 0.05°$, which corresponds to an uncertainty of ± 3.3 g/cm^2 in $X_{\max}$. The uncertainty of the analysis using the Opt-copter, considering optical aberration and GPS accuracy, was estimated to be $\pm 0.03°$.

Further studies are planned to evaluate the spot size of each FD and the effect of pointing direction shifts on the analysis of cosmic ray events.

References

[1] H. Tokuno *et al.*, "New air fluorescence detectors employed in the Telescope Array experiment," *Nucl. Instrum. Methods Phys. Res. A*, vol. 676, pp. 54–65, 2012. doi:10.1016/j.nima.2012.02.044

[2] T. Tomida *et al.*, "Development of the calibration device using UAV mounted UV-LED light source for the fluorescence detector," *EPJ Web of Conferences*, vol. 210, p. 05015, EDP Sciences, 2019. doi:10.1051/epjconf/201921005015

[3] A. Nakazawa *et al.*, "FOV direction and image size calibration of Fluorescence Detector using light source on UAV," in *Proceedings of the 37th International Cosmic Ray Conference — PoS(ICRC2021)*, vol. 395, p. 369, 2022. doi:10.22323/1.395.0369

Full Authors List: The Telescope Array Collaboration

R.U. Abbasi[1], T. Abu-Zayyad[1,2], M. Allen[2], J.W. Belz[2], D.R. Bergman[2], F. Bradfield[3], I. Buckland[2], W. Campbell[2], B.G. Cheon[4], K. Endo[3], A. Fedynitch[5,6], T. Fujii[3,7], K. Fujisue[5,6], K. Fujita[5], M. Fukushima[5], G. Furlich[2], Z. Gerber[2], N. Globus[8], T. Hanaoka[9], W. Hanlon[2], N. Hayashida[10], H. He[11*], K. Hibino[10], R. Higuchi[11], D. Ikeda[10], D. Ivanov[2], S. Jeong[12], C.C.H. Jui[2], K. Kadota[13], F. Kakimoto[10], O. Kalashev[14], K. Kasahara[15], Y. Kawachi[3], K. Kawata[5], I. Kharuk[14], E. Kido[5], H.B. Kim[4], J.H. Kim[2], J.H. Kim[2†], S.W. Kim[12‡], R. Kobo[3], I. Komae[3], K. Komatsu[16], K. Komori[9], A. Korochkin[17], C. Koyama[5], M. Kudenko[14], M. Kuroiwa[16], Y. Kusumori[9], M. Kuznetsov[14], Y.J. Kwon[18], K.H. Lee[4], M.J. Lee[12], B. Lubsandorzhiev[14], J.P. Lundquist[2,19], H. Matsushita[3], A. Matsuzawa[16], J.A. Matthews[2], J.N. Matthews[2], K. Mizuno[16], M. Mori[9], S. Nagataki[11], K. Nakagawa[3], M. Nakahara[3], H. Nakamura[9], T. Nakamura[20], T. Nakayama[16], Y. Nakayama[9], K. Nakazawa[9], T. Nonaka[5], S. Ogio[5], H. Ohoka[5], N. Okazaki[5], M. Onishi[5], A. Oshima[21], H. Oshima[5], S. Ozawa[22], I.H. Park[12], K.Y. Park[4], M. Potts[2], M. Przybylak[23], M.S. Pshirkov[14,24], J. Remington[2§], C. Rott[2], G.I. Rubtsov[14], D. Ryu[25], H. Sagawa[5], N. Sakaki[5], R. Sakamoto[9], T. Sako[5], N. Sakurai[5], S. Sakurai[3], D. Sato[16], K. Sekino[5], T. Shibata[5], J. Shikita[3], H. Shimodaira[5], H.S. Shin[3,7], K. Shinozaki[26], J.D. Smith[2], P. Sokolsky[2], B.T. Stokes[2], T.A. Stroman[2], H. Tachibana[3], K. Takahashi[5], M. Takeda[5], R. Takeishi[5], A. Taketa[27], M. Takita[5], Y. Tameda[9], K. Tanaka[28], M. Tanaka[29], M. Teramoto[9], S.B. Thomas[2], G.B. Thomson[2], P. Tinyakov[14,17], I. Tkachev[14], T. Tomida[16], S. Troitsky[14], Y. Tsunesada[3,7], S. Udo[10], F. Urban[30], A. Urena[30], M. Vrábel[26], D. Warren[11], K. Yamazaki[21], Y. Zhezher[5,14], Z. Zundel[2], and J. Zvirzdin[2]

[1] *Department of Physics, Loyola University-Chicago, Chicago, Illinois 60660, USA*
[2] *High Energy Astrophysics Institute and Department of Physics and Astronomy, University of Utah, Salt Lake City, Utah 84112-0830, USA*
[3] *Graduate School of Science, Osaka Metropolitan University, Sugimoto, Sumiyoshi, Osaka 558-8585, Japan*
[4] *Department of Physics and The Research Institute of Natural Science, Hanyang University, Seongdong-gu, Seoul 426-791, Korea*
[5] *Institute for Cosmic Ray Research, University of Tokyo, Kashiwa, Chiba 277-8582, Japan*
[6] *Institute of Physics, Academia Sinica, Taipei City 115201, Taiwan*
[7] *Nambu Yoichiro Institute of Theoretical and Experimental Physics, Osaka Metropolitan University, Sugimoto, Sumiyoshi, Osaka 558-8585, Japan*
[8] *Institute of Astronomy, National Autonomous University of Mexico Ensenada Campus, Ensenada, BC 22860, Mexico*
[9] *Graduate School of Engineering, Osaka Electro-Communication University, Neyagawa-shi, Osaka 572-8530, Japan*
[10] *Faculty of Engineering, Kanagawa University, Yokohama, Kanagawa 221-8686, Japan*
[11] *Astrophysical Big Bang Laboratory, RIKEN, Wako, Saitama 351-0198, Japan*
[12] *Department of Physics, Sungkyunkwan University, Jang-an-gu, Suwon 16419, Korea*
[13] *Department of Physics, Tokyo City University, Setagaya-ku, Tokyo 158-8557, Japan*
[14] *Institute for Nuclear Research of the Russian Academy of Sciences, Moscow 117312, Russia*
[15] *Faculty of Systems Engineering and Science, Shibaura Institute of Technology, Minumaku, Tokyo 337-8570, Japan*
[16] *Academic Assembly School of Science and Technology Institute of Engineering, Shinshu University, Nagano, Nagano 380-8554, Japan*
[17] *Service de Physique Théorique, Université Libre de Bruxelles, Brussels 1050, Belgium*
[18] *Department of Physics, Yonsei University, Seodaemun-gu, Seoul 120-749, Korea*
[19] *Center for Astrophysics and Cosmology, University of Nova Gorica, Nova Gorica 5297, Slovenia*
[20] *Faculty of Science, Kochi University, Kochi, Kochi 780-8520, Japan*
[21] *College of Science and Engineering, Chubu University, Kasugai, Aichi 487-8501, Japan*
[22] *Quantum ICT Advanced Development Center, National Institute for Information and Communications Technology, Koganei, Tokyo 184-8795, Japan*
[23] *Doctoral School of Exact and Natural Sciences, University of Łódź, Łódź, Łódź 90-237, Poland*
[24] *Sternberg Astronomical Institute, Moscow M.V. Lomonosov State University, Moscow 119991, Russia*
[25] *Department of Physics, School of Natural Sciences, Ulsan National Institute of Science and Technology, UNIST-gil, Ulsan 689-798, Korea*
[26] *Astrophysics Division, National Centre for Nuclear Research, Warsaw 02-093, Poland*
[27] *Earthquake Research Institute, University of Tokyo, Bunkyo-ku, Tokyo 277-8582, Japan*
[28] *Graduate School of Information Sciences, Hiroshima City University, Hiroshima, Hiroshima 731-3194, Japan*
[29] *Institute of Particle and Nuclear Studies, KEK, Tsukuba, Ibaraki 305-0801, Japan*
[30] *CEICO, Institute of Physics, Czech Academy of Sciences, Prague 182 21, Czech Republic*

[*] Presently at: Purple Mountain Observatory, Nanjing 210023, China
[†] Presently at: Physics Department, Brookhaven National Laboratory, Upton, NY 11973, USA
[‡] Presently at: Korea Institute of Geoscience and Mineral Resources, Daejeon, 34132, Korea
[§] Presently at: NASA Marshall Space Flight Center, Huntsville, Alabama 35812, USA

Acknowledgments

The Telescope Array experiment is supported by the Japan Society for the Promotion of Science(JSPS) through Grants-in-Aid for Priority Area 431, for Specially Promoted Research JP21000002, for Scientific Research (S) JP19104006, for Specially Promoted Research JP15H05693, for Scientific Research (S) JP19H05607, for Scientific Research (S) JP15H05741, for Science Research (A) JP18H03705, for Young Scientists (A) JPH26707011, and for Fostering Joint International Research (B) JP19KK0074, by the joint research program of the Institute for Cosmic Ray Research (ICRR), The University of Tokyo; by the Pioneering Program of RIKEN for the Evolution of Matter in the Universe (r-EMU); by the U.S. National Science Foundation awards PHY-1806797, PHY-2012934, PHY-2112904, PHY-2209583, PHY-2209584, and PHY-2310163, as well as AGS-1613260, AGS-1844306, and AGS-2112709; by the National Research Foundation of Korea (2017K1A4A3015188, 2020R1A2C1008230, and RS-2025-00556637) ; by the Ministry of Science and Higher Education of the Russian Federation under the contract 075-15-2024-541, IISN project No. 4.4501.18, by the Belgian Science Policy under IUAP VII/37 (ULB), by National Science Centre in Poland grant 2020/37/B/ST9/01821, by the European Union and Czech Ministry of Education, Youth and Sports through the FORTE project No. CZ.02.01.01/00/22_008/0004632, and by the Simons Foundation (00001470, NG). This work was partially supported by the grants of the joint research program of the Institute for Space-Earth Environmental Research, Nagoya University and Inter-University Research Program of the Institute for Cosmic Ray Research of University of Tokyo. The foundations of Dr. Ezekiel R. and Edna Wattis Dumke, Willard L. Eccles, and George S. and Dolores Doré Eccles all helped with generous donations. The State of Utah supported the project through its Economic Development Board, and the University of Utah through the Office of the Vice President for Research. The experimental site became available through the cooperation of the Utah School and Institutional Trust Lands Administration (SITLA), U.S. Bureau of Land Management (BLM), and the U.S. Air Force. We appreciate the assistance of the State of Utah and Fillmore offices of the BLM in crafting the Plan of Development for the site. We thank Patrick A. Shea who assisted the collaboration with much valuable advice and provided support for the collaboration's efforts. The people and the officials of Millard County, Utah have been a source of steadfast and warm support for our work which we greatly appreciate. We are indebted to the Millard County Road Department for their efforts to maintain and clear the roads which get us to our sites. We gratefully acknowledge the contribution from the technical staffs of our home institutions. An allocation of computing resources from the Center for High Performance Computing at the University of Utah as well as the Academia Sinica Grid Computing Center (ASGC) is gratefully acknowledged.